Eidgenössische Technische Hochschule Zürich
Swiss Federal Institute of Technology Zurich

Institut für Fluiddynamik

ETH Zentrum, ML H 33
CH-8092 Zürich

Prof. Dr. Thomas Rösgen
Sonneggstrasse 3
Telefon +41-44-632 2646
Fax +41-44-632 1147
roesgen@ifd.mavt.ethz.ch
www.ifd.mavt.ethz.ch

Power efficiency and aerodynamic forces measurements on the Dettwiler-wind turbine

Lukas Prochazka

Customer:

From May 17 until May 19 2006 measurements on the Dettwiler- wind turbine were conducted in the large subsonic wind tunnel at the Institute of Fluid Dynamics at ETH Zurich. The objectives of these tests were to quantify the power efficiency, the start and stop wind speed and the aerodynamic loads of this novel wind converter. Wind speeds up to 15m/s and three different blade sizes were considered.

1 Introduction

The most important parameter to judge an energy converting device, is the power efficiency defined as the output/ input power ratio, eq. 1.1.:

$$c_p = \frac{P_{OUT}}{P_{IN}}. \tag{1.1}$$

In an experimental investigation of the efficiency of a power plant, the output power is normally determined by measuring the power produced by the electrical generator. For the calculation of the input power usually a well defined parameter like the chemical energy content of a fuel or the illuminated area of a solar cell is used. But there are cases for which no standard definition of the input power is applicable and where a comparison of different devices becomes difficult. This problem arises for wind energy converters, where different converting techniques and designs exist.

For the case of wind energy converters, the input power is the kinetic wind energy, defined as the product of the density of the air ρ, the effective area A of the converter and the wind velocity U to the power of 3, eq. 1.2.:

$$P_{IN} = \frac{1}{2}\rho A U^3 . \qquad (1.2)$$

The effective area strongly depends on the converter type and its design. This makes the comparison of the power efficiency from different converter types difficult, especially when a new design is tested and no information can be found in literature. To define a reasonable effective area for the investigated Dettwiler-wind turbine, the effective area of an existing converter type (drag type, see below) which seems to operate similarly to the Dettwiler one, is used.

The following text gives a short summary about the two basic wind turbine working principles and their respective power efficiency computation. Based on this, a reasonable classification of the Dettwiler- wind turbine becomes possible.

Wind turbines can be classified in two main groups. Power plants which use aerodynamic lift belong to the first group and are usually called the lift-type wind turbine. Figure 1.1 (left) shows the widespread lift-type wind turbine with a 3 blade rotor. Drag driven turbines form the second group and are referred to as drag-type wind turbines. Such a turbine can be a simple cup anemometer, used for wind speed measurement (figure 1.1 centre), or a more elaborated Savonius rotor (figure 1.1 right).

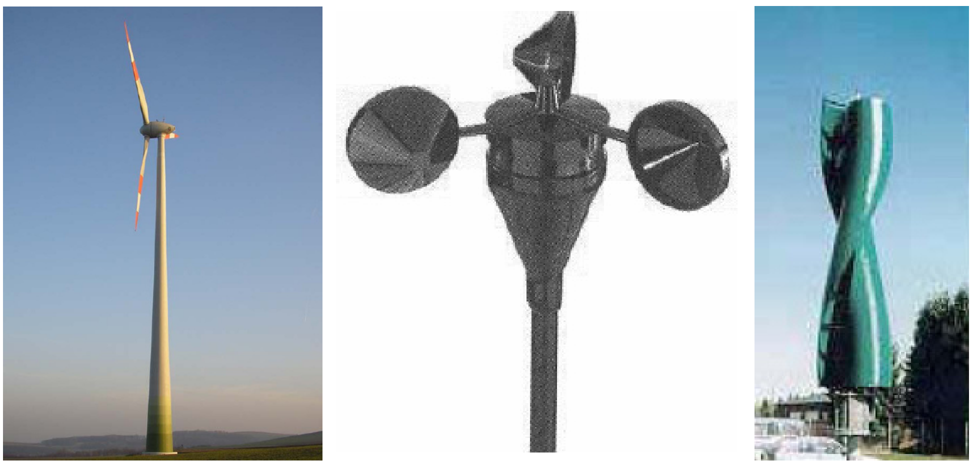

Fig 1.1: (left) Lift-type turbine with a 3 blade rotor (source: Wind Power Plants", R. Gasch & J. Twele); (middle) Drag-type wind turbine: cup anemometer (source: "Wind Energy Explained", J. F. Manwell et al.); (right) Drag-type wind turbine: Savonius rotor (source: www.eurowind-uk.net)

The lift-type turbines use wing shaped rotors where on the luff-side the fluid is accelerated and thus produces low pressure. Contrarily the fluid on the lee-side is decelerated what causes a pressure rise. Due to the pressure difference between the luff and lee-side of the rotor an aerodynamic force perpendicular to the flow, usually called the aerodynamic lift, is generated. If the angle of attack of the rotor is chosen correctly, the flow around the foil does not separate and the aerodynamic drag is much smaller than the lift force (figure 1.2). This makes the aerodynamic lift the main propelling force of such a turbine.

Lift-type wind turbines are widespread due to their high efficiency, only limited by the Betz limit which stands for the maximum possible energy conversion efficiency by any device in any free-flowing fluid stream.

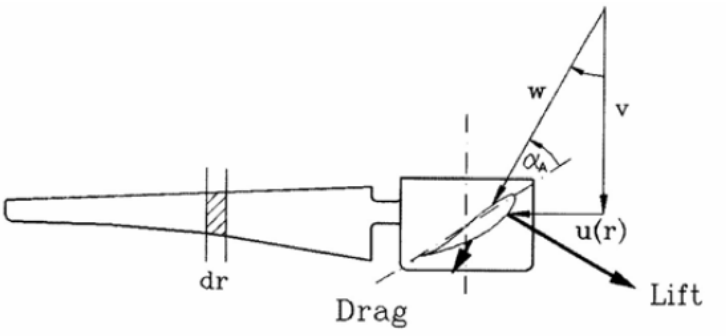

Fig. 1.2: Rotor profile and aerodynamic forces acting on rotor blade of a lift-type turbine (source: ”Wind Power Plants”, R. Gasch & J. Twele)

Accordingly to the Betz limit, maximum 60% of the total wind power can be converted into mechanical power. The energy conversion from a free-flowing fluid stream is limited because the extraction of (kinetic) energy implies a decrease of fluid velocity which cannot drop to zero. Otherwise the mass conservation would not be satisfied anymore.

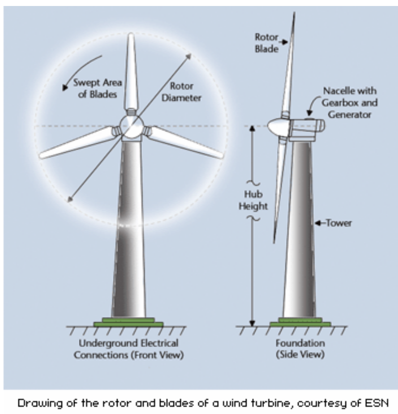

Fig. 1.3: Sketch of the swept area of lift-type wind turbine (source: www.daviddarling.info/encyclopedia)

Modern lift-type designs reach efficiencies up to 80% of the Betz limit. The effective area of lift-type turbines is defined as the swept area of the rotor.

If the aerodynamic drag is the dominant propelling force, the converter is classified as a drag-type turbine. In this case the flow around a blade separates directly at the blade edge generating a separated flow region on the lee-side of the blade. Thus the pressure on the luff-side is higher than on the lee-side of the blade. The resulting force is directed against the blade movement, the so called form drag.
The drag force D depends on the blade geometry represented by the drag coefficient c_D, the blade area A and the relative flow velocity, defined as the difference between the wind speed v and the blade velocity u (eq. 1.3 and figure 1.4). The maximum achievable efficiency with a drag-type wind turbine is principally limited by the first parameter to roughly 18%. This value is based on half spherical blades with the highest possible drag coefficient of c_D = 1.33.

$$D = c_D \frac{1}{2} \rho (v-u)^2 A \qquad (1.3)$$

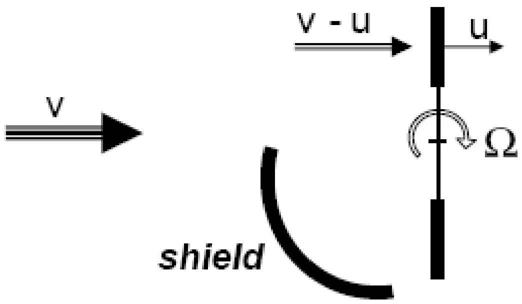

Fig. 1.4: Working principle of a drag-type wind turbine with a two blade rotor

Due to the fact that the drag force is dependent on the relative velocity and not on the absolute wind velocity, the optimum operating point depends critically on the rotor speed and the wind speed. Figure 1.5 shows the power efficiency as a function of the blade speed ratio, defined as the ratio between the blade and the wind speed. Obviously, the maximum efficiency is reached for a blade speed 3 times smaller than the wind speed. Variations from this optimum operation point lead to distinct decrease in efficiency.

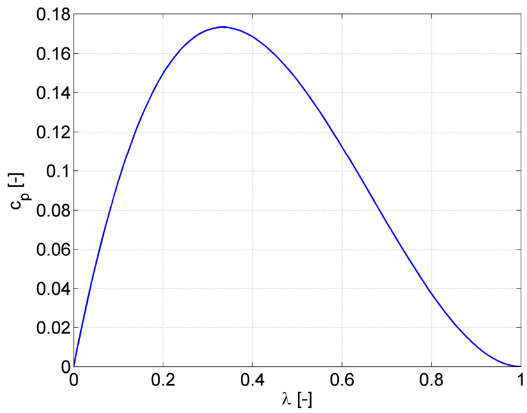

Fig. 1.5: Power efficiency as function of the blade speed ratio for a drag-type wind turbine

The effective area of a drag-type wind turbine is usually defined as the frontal area of a blade. The assumption of uniform motion of the rotor implies a constant effective area during a revolution.

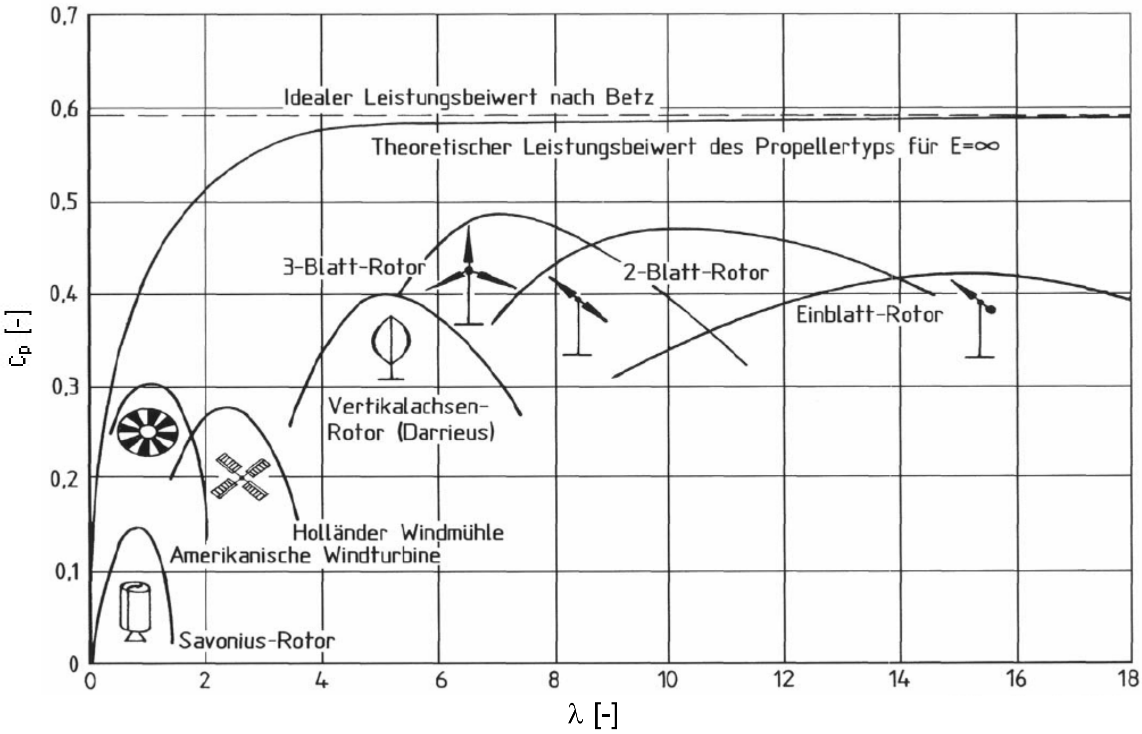

Fig. 1.6: Power efficiency and tip speed ratio of different wind turbine types

In figure 1.6 power efficiency c_p and tip speed of the rotor for different wind converter types are compared (λ defines the ratio between the rotor tip speed and the wind speed). Additionally, the Betz limit in relation to a more detailed consideration of the theoretical efficiency limit of a propeller is shown. The Savonius-rotor is the only drag-type wind turbine considered. Its much lower power efficiency - compared to a modern 3 blade lift-type - is obvious. On the other hand if noise pollution is an issue, the drag-type turbine has advantages over the lift-type one due to the much lower tip speed of the rotor.

The Dettwiler-wind turbine features two circular blades on each side of the longitudinal axis (figure 1.7). The blades are made of a rigid steel ring covered with a plastic canvas. Due to the skin of fabric, the blades are not completely flat but show a slight curvature dependent on their position relative to the wind direction. Position and orientation of the blades is given by a rotation around two axes: each blade revolves around its mounting shaft while the whole system rotates around a common horizontal axis. If the one blade is perpendicular to the wind direction the second is aligned with the flow. The two other blades on the opposite side are autonomous to adjust their relative position for a uniform motion of the turbine.

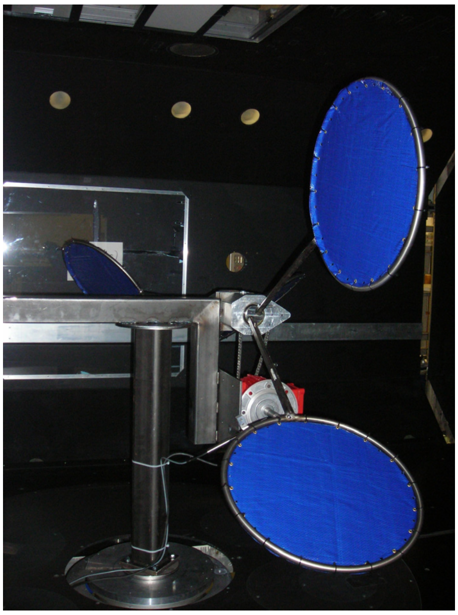

Fig. 1.7: The Dettwiler-wind turbine located within the test section of the large subsonic wind tunnel at IFD (ETHZ)

Even though the blades have a slightly curved profile and could produce aerodynamic lift, the flow behind the blade will separate at small angles of attack. The Dettwiler-wind turbine should thus be classified as a pure drag-driven machine with an effective area that equals two times the area of a single blade.

2 Testing facility

The tests on the Dettwiler-wind turbine were conducted in the large subsonic wind tunnel at the Institute of Fluid Dynamics (ETH Zurich). The wind tunnel is a closed-loop tunnel with a maximum flow velocity of 60m/s. The closed test section has a cross section of 3 x 2m^2 (width x height) and a length of around 5m (figure 2.1).

Fig. 2.1: The large subsonic wind tunnel at the Institute of Fluid Dynamics (ETHZ); (left) entry nozzle, (middle) closed test section, (right) diffuser

The wind turbine was mounted on a base plate connected to the 6-component force balance (figure 1.7). The 3 forces (x-, y-, and z-force) and the corresponding moments (M_x, M_y and M_z) were measured. Additionally, flow velocity and the temperature in the test section were recorded.

The rotational speed of the generator was measured with an optical sensor. From this, the speed of the rotor was calculated by dividing the generator speed by the total transmission ratio of 20.3.

To allow the measurement of the electrical power output under varying loads a potentiometer with a maximum resistance of approximately 28 Ohm (0% load) was used. The electrical current through the resistance was measured with an additional shunt resistance. The output voltage was kept below the 10 Volt limit of the data acquisition system with a voltage divider. With the DC output of the generator, a data acquisition rate of 10Hz was found to be sufficient.

Fig. 2.2: Equipment for electrical power measurement; potentiometer (left on the table), processing unit for rotation speed measurement (right on the table)

All data was sampled at a rate of 10Hz using a MGCplus (HBM) data acquisition system. Electronic filters were used which were matched to the sample rate in order to fulfil the Nyquist criterion. The data was stored in ASCI format and post-processed with Matlab software.

3 Description of the measured configurations

Besides measurements at wind speeds between 0 and 15m/s with electrical loads between 0% (28Ohm) and ≈ 90% (≈ 3Ohm), blades of three different dimensions have been tested. The smallest blade had a cross section of $0.2m^2$, the next larger an area of $0.35m^2$ and the largest had an area of $0.5m^2$. The distance between the centre of area of a blade and the rotation centre was the same for all mentioned configurations (figure 3.1).

It has to be mentioned that especially in the case with the largest blades the distance between the outer edge of the blades and the wind tunnel wall was only 30cm. This distance is too small to avoid any influences on the rotor due to the wall proximity. Due to the tight schedule this effect was not investigated.

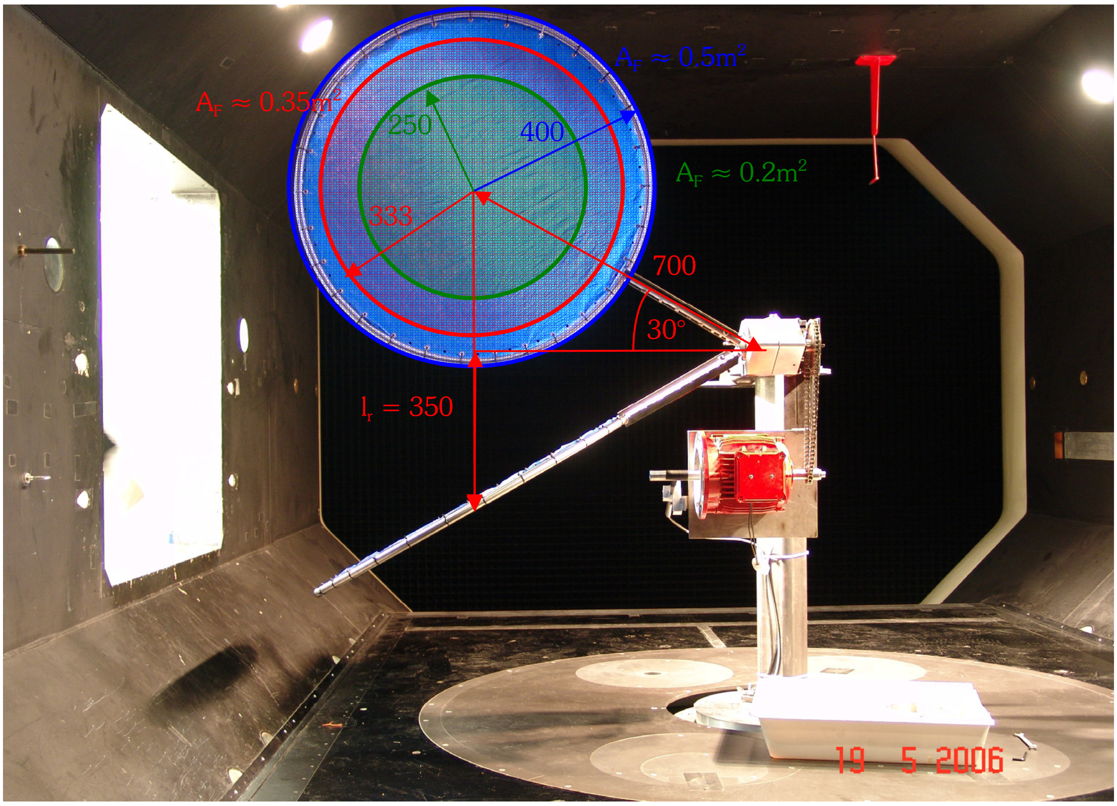

Fig. 3.1: Blade dimensions and geometrical blade arrangement. (It has to be mentioned that the opposing blades are not fixed in this image)

Table 3.1 summarizes all test runs and gives information about the parameters and the measurement procedure:

Nr.	Wind speed [m/s]	Blade area [m2]	Load [%]	Notes
		Day 1		
1	12	0.2	variable	
2	12	0.2	variable	Repetition of Nr. 1
3	15	0.2	variable	
4	10	0.2	variable	
5	8	0.2	variable	
6		0.2	0%	min. velocity at start min. velocity when stops
7		0.2	50%	min. velocity at start min. velocity when stops
8		0.2	30%	min. velocity at start min. velocity when stops
9	10	0.35	variable	
10	12	0.35	variable	
11	8	0.35	variable	
12	7	0.35	variable	
13	11	0.35	variable	
14		0.35	100%	min. velocity at start min. velocity when stops
15		0.35	50%	min. velocity at start min. velocity when stops
16		0.35	30%	min. velocity at start min. velocity when stops
17	0 - 12	0.35		Blocked rotor => drag measurement if blade is perpendicular to the wind direction
18		0.5	100%	min. velocity at start min. velocity when stops
19		0.5	50%	min. velocity at start min. velocity when stops
		Day 2		
20	12	0.5	variable	
21	11	0.5	variable	
22	10	0.5	variable	
23	9	0.5	variable	
24	8	0.5	variable	
Premature test termination due to a failure within the gearbox!!				

Table 3.1: Conducted test runs

4 Measurement procedure

Prior to each test run a wind-off measurement was accomplished to correct a possible signal offset in the real data.

For the measurements, the data acquisition was started after the wind speed was set and the rotational speed of the generator was adjusted to the allowable maximum of 1500min^{-1}. The flow velocity was controlled electronically trough the rotational speed of the wind tunnel fan. The rotational speed of the generator was adjusted by varying the electrical load (potentiometer).

Each measurement started at 0% load (28Ohm). Only if the corresponding generator speed exceeded the allowable value, the initial value was higher. By reducing the electrical resistance, the load was then steadily increased to a maximal load of around 3Ohm or to a load where the rotor came to rest. Afterwards, the load was again decreased down to the initial load.

Beside the common power measurements, tests were also conducted to find both the minimum wind speed to start the turbine and the wind speed where the turbine stops. For this purpose the electrical load was adjusted to a constant value and the wind speed was continuously increased from zero to where regular rotation set in. Afterwards, the wind speed was slowed down until the rotor came to a rest.

5 Post processing of the measured data

Based on literature the efficiency of the Dettwiler-wind turbine can be expressed using the power coefficient or the power efficiency c_p as defined in equation 1.1 and 1.2. The effective area equals two times the area of a single blade. The power coefficient is a function of the electrical load and a function of the blade speed ratio λ. The electrical load is defined as the ratio of the effective and the maximum electrical resistance (here 28Ohm) expressed in %, eq. 5.1.

$$Load = \left(1 - \frac{R}{R_{\max}}\right) 100\% \qquad (5.1)$$

The blade speed ratio λ is defined as the ratio between the blade and the wind speed. The blade speed is the product of the angular velocity of the rotor ω_{rotor} or its rotation speed n_{rotor}, respectively and the distance between the rotational axis and the centre of area of the blade l_r (for all blade configurations l_r = 350mm, see figure 3.1), eq. 5.2.

$$\lambda = \frac{U_{blade}}{U_{wind}} = \frac{\omega l_r}{U_{wind}} = \frac{\pi}{30} \frac{n_{rotor} l_r}{U_{wind}} \qquad (5.2)$$

To see if the efficiency scales with the blade size, the power coefficient is computed as a function of Reynolds number as well. The Reynolds number is defined as follows, eq. 5.3.

$$\mathrm{Re} = \frac{U_{wind} D_{blade}}{\nu} \qquad (5.3)$$

U_{wind} represents the wind speed, D_{blade} the blade diameter and ν the kinematic viscosity of air (ν = 1.5*10^{-5} m^2/s).

The measured aerodynamic forces and moments are all shown as a function of the electrical load (here equivalent to the rotor speed) or as a function of the Reynolds number. The forces F and moments M are normalized with the corresponding dynamic pressure ($1/2\rho U^2$) and the effective area to obtain the force and moment coefficients ($c_{F(M)}$), respectively, eq. 5.4. In some cases the aerodynamic loads are normalized using the dynamic pressure alone ($C_{F(M)}$), eq. 5.5.

$$c_F = \frac{F}{\frac{1}{2}\rho U^2 A} \quad [-] \quad \text{or} \quad c_M = \frac{M}{\frac{1}{2}\rho U^2 A} \quad [\mathrm{m}] \qquad (5.4)$$

$$C_F = \frac{F}{\frac{1}{2}\rho U^2} \quad [\mathrm{m}^2] \quad \text{or} \quad C_M = \frac{M}{\frac{1}{2}\rho U^2} \quad [\mathrm{m}^3] \qquad (5.5)$$

For a better interpretation of the forces and moments the chosen sign convention is shown in figure 5.1.

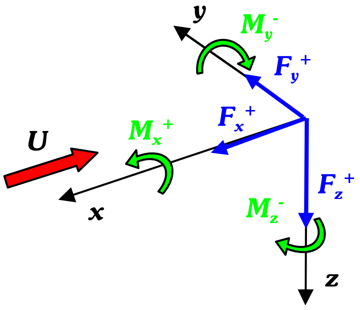

Fig. 5.1: Sign convention for the measured forces and moments

For the current study, any dynamic effects due to a non uniform motion of the rotor are neglected. To compensate this and to reduce measurement noise, the raw data is time averaged over 50 data points.

In the c_p representation a polynomial is fitted to the time averaged data. Depending on subjective appraisement, up to forth-order polynomials were chosen.

6 Results

Operating map of the Dettwiler-wind turbine

Figure 6.1 shows the power efficiency c_p as a function of the electrical load for all three blade sizes and the considered wind speeds, table 3.1. Each curve shows the data for a constant wind speed. The arrows indicate increasing wind speed. Due to the limited maximum rotor speed ($1500 min^{-1}$) some measurements were started with an increased load.

Generally the power efficiency decreases with increasing load. If the configuration with the largest blades is considered, dependent on the wind speed a maximum efficiency is already reached between 30 and 50% load. There is no indication for an efficiency decrease towards lower loads. For the two smaller blades sizes and at lower wind speeds a maximum efficiency is only reached for zero loading.

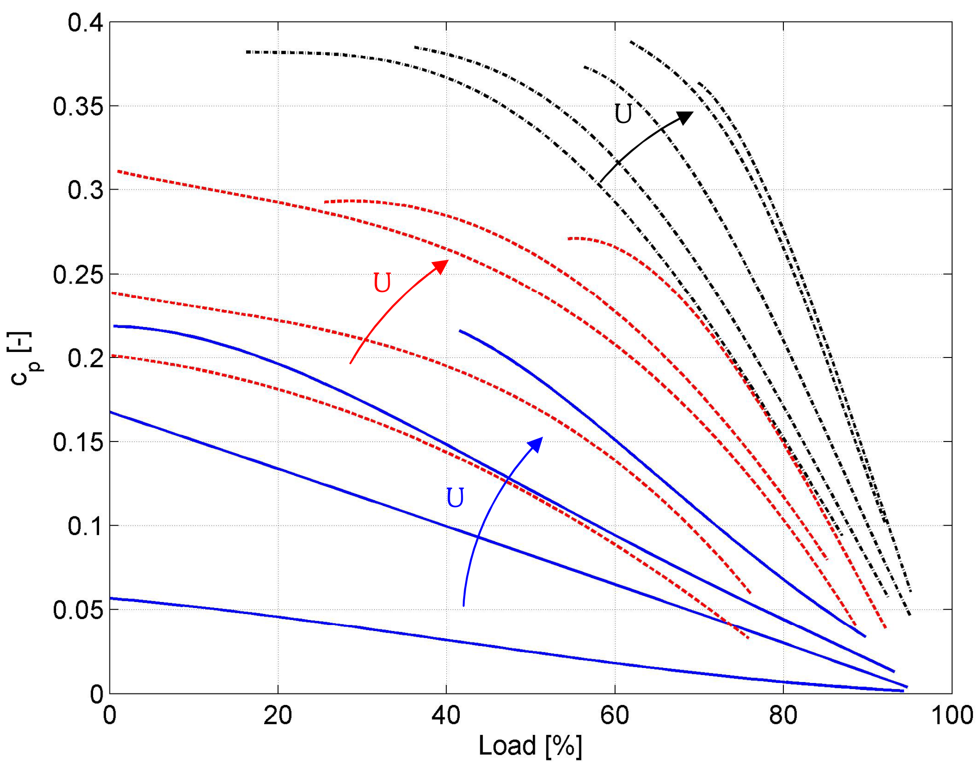

Fig. 6.1: Power efficiency as a function of electrical load for the 3 blade sizes and different wind speeds. solid: $A_b = 0.2m^2$, U = 8, 10, 12 and 15m/s; dotted: $A_b = 0.35m^2$, U = 7, 8, 10, 11 and 12m/s; dashed: $A_b = 0.5m^2$, U = 8, 9, 10, 11 and 12m/s

It is interesting to note that already with the smallest blades efficiencies above 20% are reached for low electrical loads and at wind speeds above 12m/s. With increasing the blade size the efficiency increases. For the largest blades even at low wind speeds (around 8m/s) and semi load values up to 40% are reached. Such high efficiencies contradict the theoretical maximum efficiency limit of about 18% for a drag-type wind turbine (figure 1.5). A possible reason for this inconsistency is discussed in chapter 7.

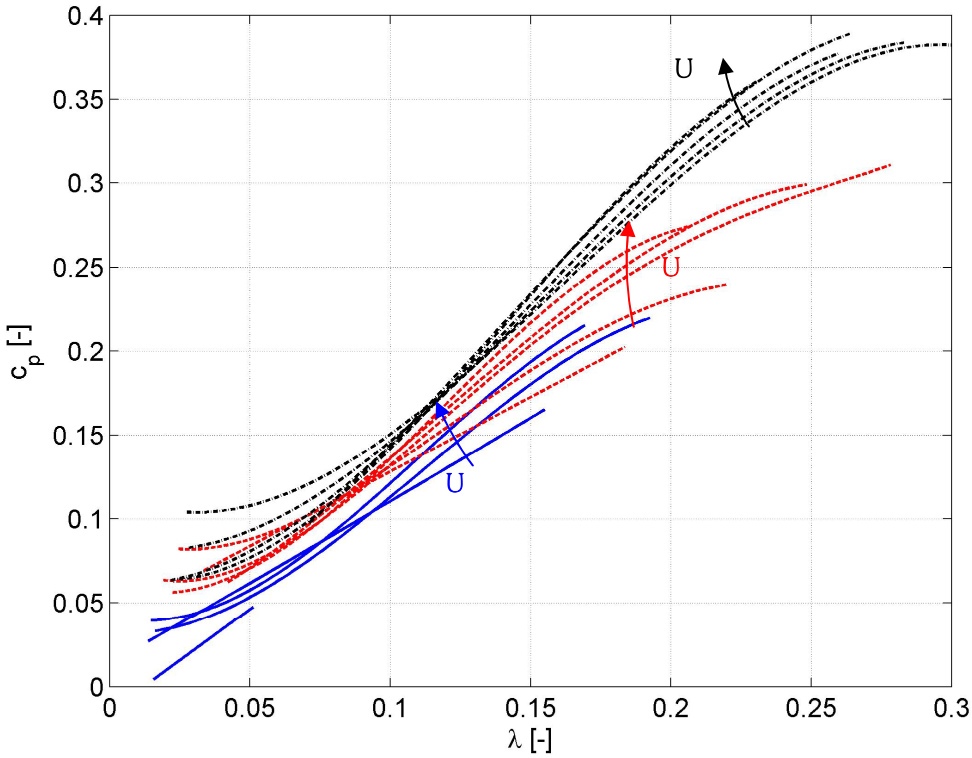

Fig. 6.2: Power efficiency as a function of the blade speed ratio for the 3 blade sizes and different wind speeds. solid: A_b = 0.2m^2, U = 8, 10, 12 and 15m/s; dotted: A_b = 0.35m^2, U = 7, 8, 10, 11 and 12m/s; dashed: A_b = 0.5m^2, U = 8, 9, 10, 11 and 12m/s

Figure 6.2 shows the power coefficient as a function of the blade speed ratio λ. Similar to figure 6.1, all blade sizes and wind speeds are considered in the chart.

Compared with the theoretical characteristics of the c_p-λ relationship for a drag-type wind turbine (figure 1.5), a qualitative agreement is obvious. As mentioned before the Dettwiler-turbine has a much higher efficiency than a conventional drag driven turbine. Probably due to energy losses in the gearbox and the generator used the blade speed ratio is limited to 0.3 and the region beyond with a decreasing c_p (figure 1.5) can not be reached with the present setup.

In figure 6.3a)- d) the power efficiency at working points for 50% (fig. 3a), 60% (fig. 3b), 70% (fig. 3c) and 80% load (fig. 3d) as a function of the Reynolds number is shown. The triangles represent the largest, the squares the medium and the circles the smallest blade area.

Obviously, there is no unambiguous correlation between the power coefficient and the Reynolds number but there is a distinct linear dependency of the wind speed on the c_p (along the linear fit the Reynolds number is proportional to the wind speed). For one blade size, the slope is approximately constant for different operation points.

It seems as if the blade size has a much higher influence on the efficiency than the wind speed.

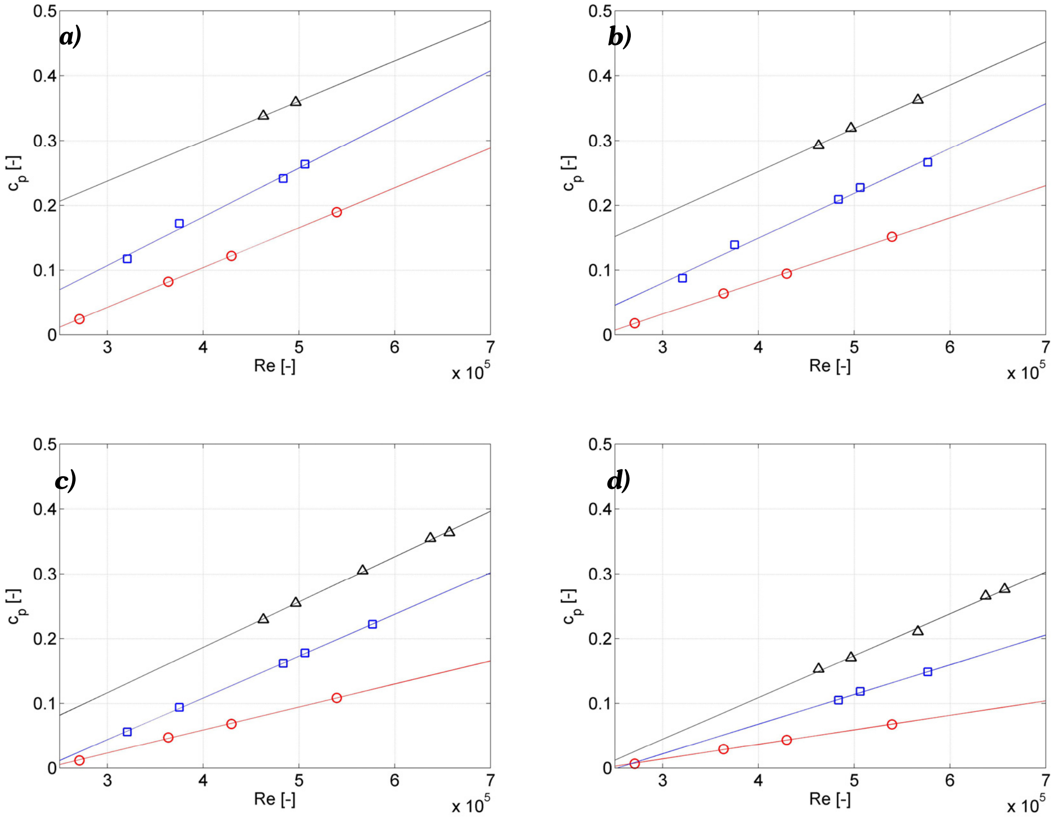

Fig. 3: Power efficiency as a function of Reynolds number; a) 50% load, b) 60% load, c) 70% load, d) 80% load; triangle: A_b = 0.5m^2, square: A_b = 0.35m^2, circle: A_b = 0.2m^2

Wind speed at turbine start and stop

Figure 6.4 represents the wind speeds at which the turbine starts to rotate and comes to rest, respectively. The investigation took place at loads of 0%, 50% and 67%. With the largest blades the highest load was omitted.

The circles symbolize the rotor configuration with the smallest, the squares with the medium and the triangle with the largest blade areas. The filled symbols represent the wind speed where the rotor comes to rest and the empty ones when the rotor starts to rotate.

The turbine with the largest blades starts to rotate at a wind speeds of around 4.5 m/s and stops below 3.5m/s. If the start and stop wind speeds for the three blade configurations are compared, it seems that the limiting wind speed increases disproportionately with a decreasing blade area.

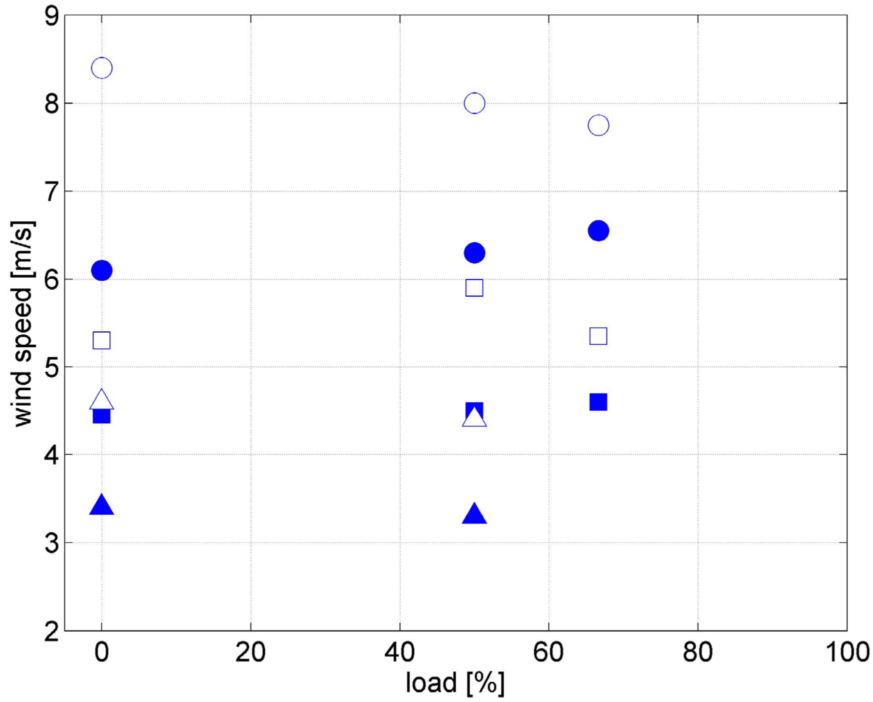

Fig. 6.4: Wind speed at rotor start and stop; circle: A_b = 0.2m^2, square: A_b = 0.35m^2, triangle: A_b = 0.5m^2, filled: wind speed at rotor stop, empty: wind speed at rotor start

Before the rotor starts to rotate no current is flowing and thus no influence of the load on the start wind speed should be observable. The still existing variations in the measured data could arise due to the different initial blade positions. The dependency of the stop velocity on the load is noticeable.

Aerodynamic forces and moments

Due to the finite number of blades a uniform motion of the turbine is not given. During one revolution the effective blade area varies. This can be observed if the time series of the drag force is plotted, figure 6.5. The measurements represent the configuration with the largest blades (A_b = 0.5m^2) at wind speeds of 12m/s. A mean aerodynamic load of approximately 220N and a dynamic part of up to 10% are measured. It has to be mentioned that compared to the drag all other loads can be neglected.

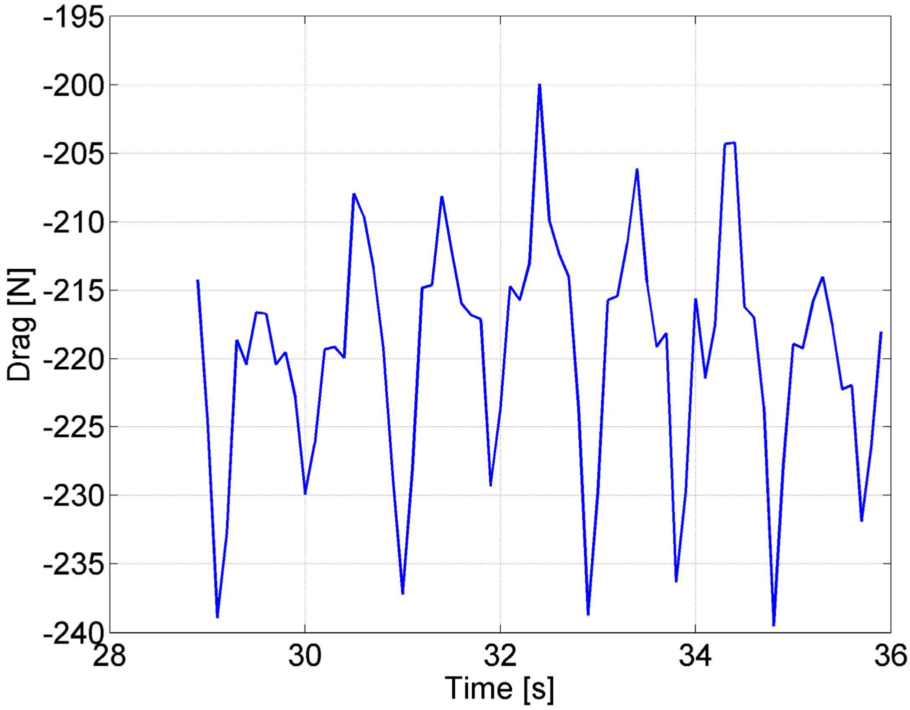

Fig. 6.5: Time varying drag of the wind turbine; Blade configuration with A_b = 0.5m^2 at wind speed U_{wind} = 12m/s

Figure 6.6a shows the time averaged drag for a rotor speed between 35 and 65rpm. In figure 6.6b the standard deviation of the drag which is a measure for its dynamic variation and thus for the uniformity of the rotor motion is shown.

If the electrical load on the turbine is decreased, the speed of the rotor will increase resulting in a reduced relative flow velocity, eq. 1.3. In figure 6.6a the drag is thus decreasing with decreasing load. An other consequence of an increasing rotor speed is an improved uniformity of the rotor motion, figure 6b. The dynamic drag variations decrease from approximately 10% at low rotor speed to about 5% at maximum rotation speed.

To investigate the effect of the wind speed and the electrical load on the drag, the force data for different wind speeds and with three different blade sizes is considered (figure 6.7, eq.5.5). The data is normalized with the dynamic pressure and is plotted against the electrical load. It has to be mentioned that the represented drag coefficient is not normalized with the effective frontal area of the wind turbine and thus has the unit of square meter.

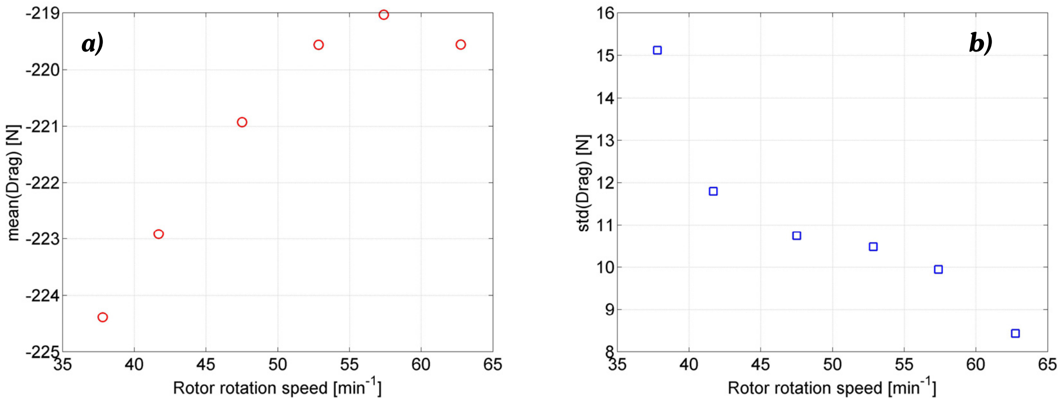

Fig. 6.6: Time averaged drag and its standard deviation as function of the rotor speed; A_b = 0.5m^2, U_{wind} = 12m/s

The large difference between the drag coefficients for the different blade sizes is mainly a consequence of the different blade areas. For the smallest blade size no influence of the electrical load and the wind speed on the drag coefficient can be observed.

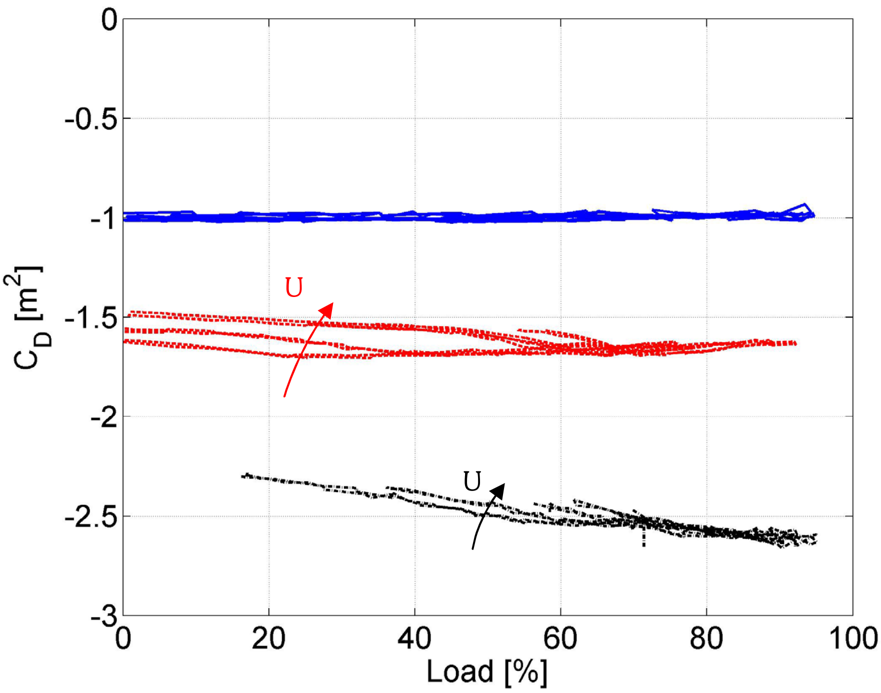

Fig. 6.7: Drag coefficient as a function of the electrical load for the 3 blade configurations and different wind speeds. Solid: A_b = 0.2m^2, U = 8, 10, 12 and 15m/s; Dotted: A_b = 0.35m^2, U = 7, 8, 10, 11 and 12m/s; Dashed: A_b = 0.5m^2, U = 8, 9, 10, 11 and 12m/s

With increasing blade size a dependency becomes more and more distinct. The drag increases with increasing load. One possible explanation could be the influence of the test section walls on the blade aerodynamics which becomes more important the larger the blades are. Because the drag force is the dominant powering force of the Dettwiler-turbine, the efficiency would possibly be higher without wall effects.

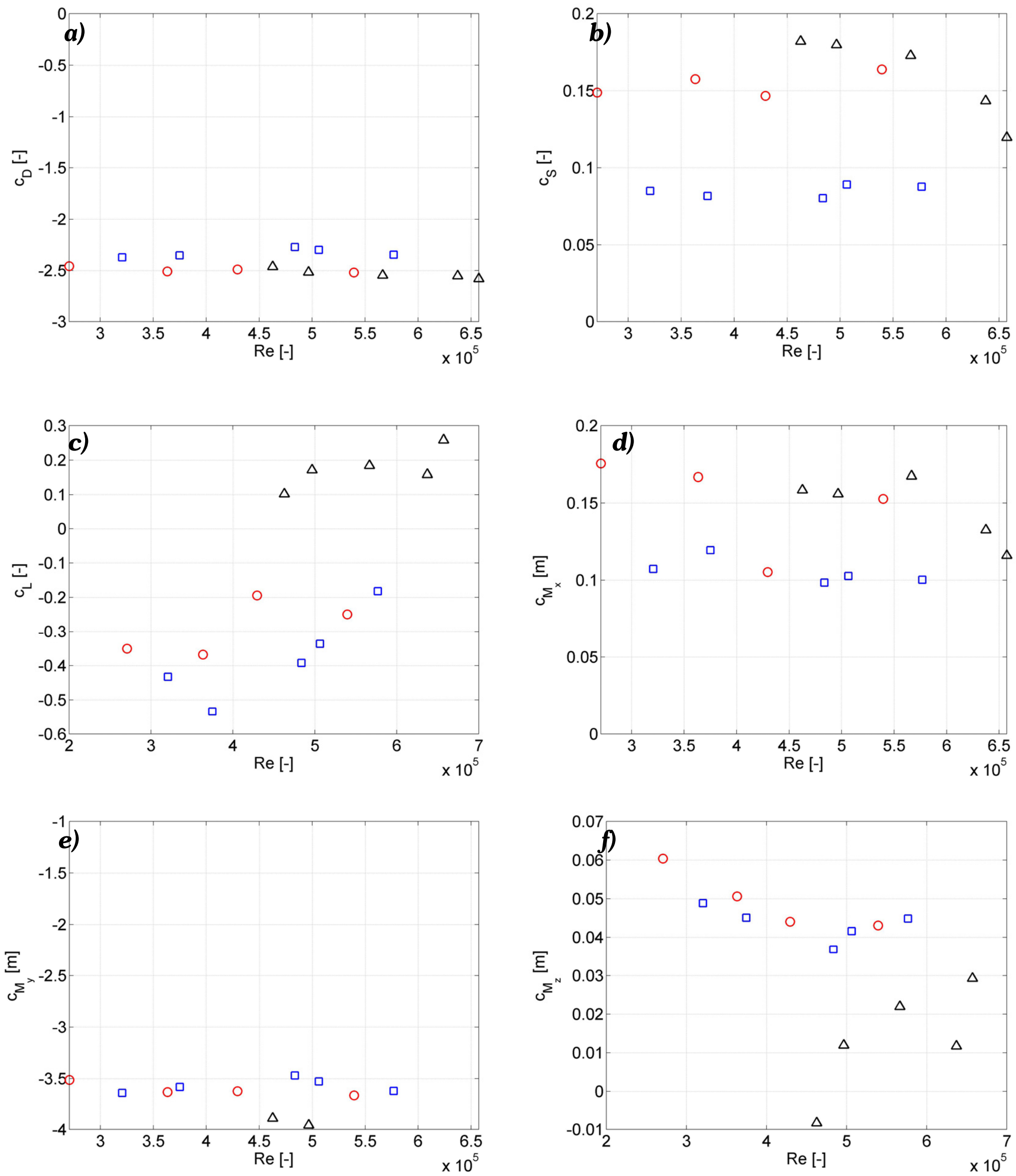

Fig. 6.8: Force and moment coefficients (time averaged) as a function of the Reynolds number; circle: $A_b = 0.2m^2$, square: $A_b = 0.35m^2$, triangle: $A_b = 0.5m^2$; a) F_x, b) F_y, c) F_z

In figure 6.8 an overview of the time averaged forces and moments as a function of the Reynolds number is given. The data has been normalized using the dynamic pressure and the total blade area, eq. 5.4.

As it is obvious in figure 6.8a the drag coefficient remains almost constant over the considered Reynolds number range at 2.5. Thus if the certain Reynolds number lies within the considered range, an estimate of the aerodynamic loading can be given for all blade sizes and wind speeds. Because the moment with respect to the y-axis is mainly due to the drag, a similar behaviour is obvious in figure 6.8e.

The side force and the corresponding moment with respect to the z-axis are small and originate probably in a slight asymmetry of the device or in a small deviation of the longitudinal axis of the turbine from the wind direction, figure 6.8b and f.

The vertical force is small and its direction is not well defined, figure 6.8c.

7 Conclusion

It seems that with the Dettwiler-wind turbine power efficiencies up to 40% are possible (turbine configuration with $A_b = 0.5m^2$). This exceeds the theoretical limit of a drag-type wind turbine by a factor of two and is similar to the efficiency of a lift-type turbine.

The reason why the Dettwiler-turbine is not limited to the theoretical efficiency of a drag-type turbine is not clear at this point and would require a detailed theoretical and experimental investigation.

However, one possible explanation could be as follows. If the effective frontal blade area of a turbine is averaged over a quarter turn of the rotor, the Dettwiler-turbine has a frontal area which is larger by a factor 1.4 than for the conventional drag-type (figure 7.1). Because the efficiency computation is based on the effective area of a conventional drag-driven turbine, the input wind power for the Dettwiler-turbine was too small.

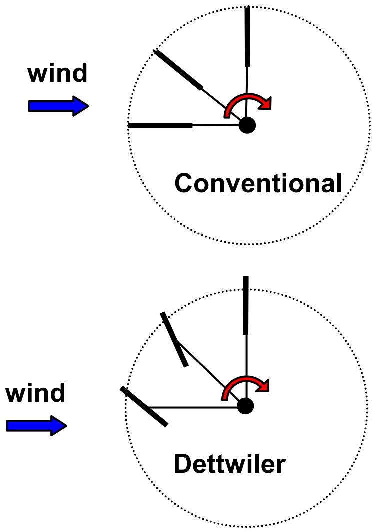

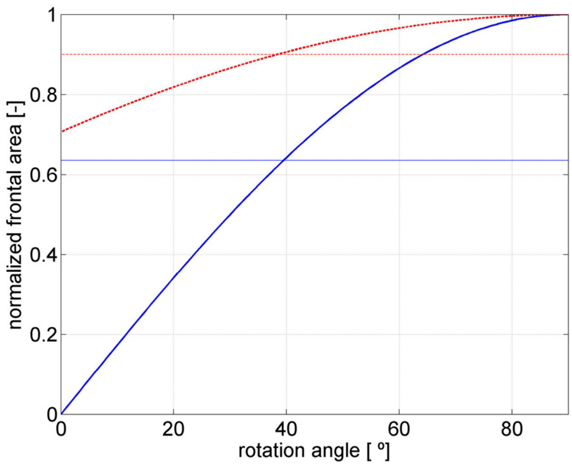

Fig. 7.1: Comparison of the frontal area averaged over a quarter rotor revolution for a conventional drag-type turbine (solid) and the Dettwiler-turbine (dashed).

Besides the mentioned quantitative discrepancy between the power efficiency of a conventional drag-type turbine and the Dettwiler-turbine, a qualitative agreement with the c_p-behaviour for a varying blade speed ratio is given.

If we consider the configuration with the largest blades, the turbine starts to rotate at a wind speed of approximately 4.5m/s and stops if the wind is slowed down to 3.5m/s. An improved gear box and a highly efficient electrical generator the wind speed limit could be reduced further.

The uniformity of rotor motion depends on the rotor speed and the dynamic component of the aerodynamic load can reach values between 10% at low rotor speed and 5% at high rotor speed.

The dominant aerodynamic load acts against the flow direction and can be interpreted as drag. The drag coefficient shows no dependency on Reynolds number within the considered range and has a value of 2.5. At wind speeds of 12m/s the configuration with the largest blades produces an aerodynamic load of approximately 200N.